

Synthesis and Characterization of Isobutylene-Based Ammonium and Phosphonium Bromide Ionomers

J. Scott Parent,^{*,†} Anca Penciu,[†] Sergio A. Guillén-Castellanos,[†] Andrea Liskova,[†] and Ralph A. Whitney[‡]

Department of Chemical Engineering and Department of Chemistry, Queen's University, Kingston, Ontario, Canada K7L 3N6

Received April 29, 2004; Revised Manuscript Received July 26, 2004

ABSTRACT: The preparation of isobutylene-based ionomers through displacement of halide from brominated poly(isobutylene-*co*-isoprene) (BIIR) by triphenylphosphine (PPh₃) and *N,N*-dimethyloctylamine (DMOA) is demonstrated. While the resulting phosphonium and ammonium bromide salts (IIR-PPh₃Br and IIR-NR₃Br, respectively) possess dynamic mechanical properties that are comparable to thermoset vulcanizates, the elastomeric network is the result of ion-pair aggregation. Evidence of intra- and intermolecular aggregation provided by dynamic mechanical and dilute solution viscosity analyses is reinforced by studies of ¹H NMR spin–spin relaxation, which demonstrate the reduced mobility of those polymer chain segments proximal to the phosphonium bromide functionality within IIR-PPh₃Br.

Introduction

Isobutylene-based elastomers are valued for their exceptional air impermeability, superior oxidative stability, and unique dynamic properties. However, the incompatibility of cationic isobutylene polymerizations with most polar monomers prohibits the direct synthesis of functional derivatives of these materials. Therefore, postpolymerization chemical modification often provides the most direct route to isobutylene-rich ionomers.¹ Brominated poly(isobutylene-*co*-isoprene) is a flexible template material for this approach, given the susceptibility of the 1–2 mol % of allylic bromide functionality within BIIR toward nucleophilic substitution.^{2,3}

We have prepared a new class of elastomeric ionomers by the displacement of bromide from BIIR by triarylphosphine and trialkylamine nucleophiles. Given the low polarity of polyisobutylene (dielectric constant, $\epsilon = 2.38$), the phosphonium and ammonium bromide functionality introduced by these substitutions are expected to be poorly solvated by the polymer matrix, leading to ion-pair aggregation that restricts polymer chain mobility⁴ and establishes a labile analogue of thermosetting vulcanization networks.⁵ In this report we present details of solvent-free ionomer syntheses involving reactions of BIIR with triphenylphosphine (PPh₃) and *N,N*-dimethyloctylamine (DMOA). Evidence of ion-pair aggregation in the solid state is provided by dynamic mechanical analysis, while aggregation in solution is characterized by viscometry. These data are correlated to restrictions of ion-pair mobility by spin–spin ¹H NMR relaxation measurements.

Experimental Section

Materials. Brominated 2,2,4,8,8-pentamethyl-4-nonene (BPMN, **1**)⁶ and (*E/Z*)-*N,N*-dimethyl-*N*-octyl-6,6-dimethyl-2-(2,2-dimethylpropyl)hept-2-enylammonium bromide (**3**)³ were prepared as previously described. The following reagents were used as received from Sigma-Aldrich (Oakville, Ontario): *N,N*-

dimethyloctylamine (DMOA, 97%), triphenylphosphine (PPh₃, 99%). BIIR (Bayer BB2030) was used as supplied by Bayer Polymers (Sarnia, Ontario).

Synthesis and Isolation of [(2*E,Z*)-6,6-Dimethyl-2-neopentylhept-2-enyl](triphenyl)phosphonium Bromide. BPMN (0.050 g, 0.18 mmol), triphenylphosphine (0.044 g, 0.17 mmol), and toluene (0.4 mL) were sealed in a 1 mL Wheaton vial and heated to 100 °C for 1 h. Volatile components were removed by Kugelrohr distillation (*P* = 0.6 mmHg, *T* = 60–70 °C, *t* = 1 h) to yield a colorless residue. High-resolution MS analysis; required for C₃₂H₄₂BrP *m/e* 537.3023; found *m/e* 537.3024. FT-IR analysis: 1437 (P–CH₂), 1111 (P–Ph), 722 (P–Ph) cm^{−1}. ¹H NMR (CDCl₃): δ 0.8–2.2 (m, 2 \times –C(CH₃)₃, 3 \times –CH₂–). Found for *E*-isomer: ¹H NMR (CDCl₃): δ 4.38 (d, –CH₂–P–Ph), 5.49 (m, H–C=). ³¹P NMR (CDCl₃): +22.25 ppm. Found for *Z*-isomer: ¹H NMR (CDCl₃): δ 4.19 (d, –CH₂–P–Ph), 5.39 (m, H–C=). ³¹P NMR (CDCl₃): +19.84 ppm. 2D COSY ¹H NMR and ROESY ¹H NMR were used to differentiate *E* and *Z* isomers.

Synthesis of IIR-NR₃Br. BIIR (50 g) was mixed with DMOA (6.3 g, 0.04 mol, 4.0 equiv with respect to allylic bromide) at 30 °C using a Haake PolyLab R600 internal batch mixer. Aliquots of the mixture (5 g) were reacted in the cavity of an Alpha Technologies advanced polymer analyzer at the desired temperature (100 and 140 °C) using an oscillation arc of 3° and a frequency of 100 cpm. Downfield ¹H NMR (CDCl₃): δ 3.24–3.37 ppm (broad d, (CH₃)₂–N–, *E/Z*), δ 3.44–3.52 and 3.61–3.71 ppm (m, –N–CH₂–(CH₂)₇–, *E/Z*), δ 3.92–4.09 ppm (s, =CR–CH₂–N–), δ 5.81–5.9 and 6.06–6.12 ppm (broad triplet, =CH–). *T*_g = –70 °C. The notation used for these ionomers is IIR-NR₃Br-*x,y*, where *x,y* denotes the mole percent of ammonium bromide functionality.

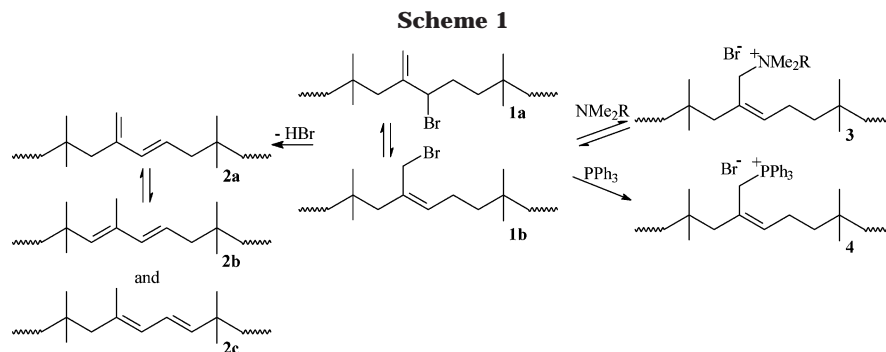
Products derived from reaction dynamics experiments were quantified by the integration of normalized ¹H NMR spectra to an estimated accuracy of $\pm 5\%$: δ 4.02–4.04 ppm (=CR–CH₂–Br, 2H, s), 3.23–3.37 ppm (*E,Z* (CH₃)₂–NRBr, 12H, s), 5.00–5.02 ppm (exo-allylic bromide, 1H, s), 5.90–6.02 ppm (conjugated dienes, 1H).

Synthesis of IIR-PPh₃Br. BIIR (50 g) was mixed with PPh₃ (7.8 g, 0.03 mol, 3.0 equiv) and reacted as described for IIR-NR₃Br. Downfield ¹H NMR (CDCl₃). For *Z* isomer: δ 4.31–4.46 ppm (broad d, =CR–CH₂–PPh₃Br), δ 5.34–5.43 ppm (broad s, =CH–CH₂–PPh₃Br). For *E* isomer δ 4.57–4.66 (broad d, =CR–CH₂–PPh₃Br), δ 5.58–5.66 (broad s, =CH–CH₂–PPh₃Br). *T*_g = –64 °C. The notation used for these ionomers is IIR-PPh₃Br-*x,y*, where *x,y* denotes the mole percent of phosphonium bromide functionality.

[†] Department of Chemical Engineering.

[‡] Department of Chemistry.

* Author for correspondence: phone (613) 533-6266; fax (613) 533-6637; e-mail parent@chee.queensu.ca.



Products of the alkylation dynamics experiments were quantified by the integration of normalized ^1H NMR spectra to an estimated accuracy of $\pm 5\%$: δ 4.02–4.04 ppm ($=\text{CH}-\text{CH}_2-\text{Br}$, 2H, s), 4.29–4.45 and 4.53–4.68 ppm (E and Z $=\text{CH}-\text{CH}_2-\text{PPh}_3\text{Br}$, 2H, d), 5.00–5.02 ppm (exo-allylic bromide, 1H, s), 5.90–6.02 ppm (conjugated dienes, 1H).

Instrumentation and Analysis. NMR spectra were recorded with a Bruker AM-500 spectrometer (500.13 MHz ^1H) in CDCl_3 , with chemical shifts referenced to tetramethylsilane. Low-resolution mass spectra were recorded with a Fisons VG Quattro triple-quadrupole instrument with chemical ionization ($i\text{-C}_4\text{H}_{10}$). High-resolution MS was performed using a Kratos MS-50 TCTA instrument operating with chemical ionization ($i\text{-C}_4\text{H}_{10}$) at the University of Montreal.

The viscosity of a given polymer solution was measured at 27 $^\circ\text{C}$ within a thermostated bath using a Canon-Fenske viscometer that yielded an elution time greater than 200 s, thereby eliminating the need for kinetic energy corrections. Data acquired in the dilute solution region (below 1.0 g/dL) were fit to Huggins' equation $\eta_{\text{red}} = [\eta] + k_H[\eta]^2c$, where $[\eta]$ is the intrinsic viscosity, c is the polymer concentration, and k_H is the empirical Huggins' parameter.⁷

Ionomer samples for DMA analysis were thermoformed by compression-molding at 100 $^\circ\text{C}$ for 40 min, whereas ZnO-cured BIIR samples were cross-linked by compression-molding at 160 $^\circ\text{C}$ for 90 min. The storage (G') and loss moduli (G'') were measured between -100 and 95 $^\circ\text{C}$ at a temperature ramp rate of 5 $^\circ\text{C}/\text{min}$ using a controlled-stress rheometer (Rheologica ViscoTech) operating in the torsion mode. Measurements were made at 1% strain and a frequency of 1 Hz.

^1H NMR Relaxation Measurements. Spin–lattice relaxation time (T_1) measurements were obtained using an inversion recovery pulse sequence ($180^\circ - t - 90^\circ$). Spin–spin relaxation times (T_2) were obtained using a Carr–Purcell–Meiboom–Gill sequence. In all cases, relaxation delays greater than $5T_1$ were used. Relaxation time constants were extracted from the time-evolution data using a nonlinear, least-squares regression algorithm.

Results and Discussion

Ionomer Structure. The exo-methylene allylic bromide (**1a**) within BIIR is a kinetically favored bromination product that can rearrange at elevated temperatures to more stable (E,Z)-endo (**1b**) isomers (Scheme 1).^{6,8} HBr elimination to yield conjugated dienes (**2a–c**) also proceeds in competition with nucleophilic substitution, thereby lowering the conversion of allylic bromide to the desired ion pair and sequestering amine (and, to a much lesser extent, phosphine) as a hydrobromide salt. The synthesis of BIIR-derived ionomers must, therefore, be concerned with the relative rates of halide substitution and dehydrobromination.

The phosphonium bromide salt derived from the reaction of PPh_3 with a suitable model compound (brominated 2,2,4,8,8-pentamethyl-4-nonene, BPMN) is structurally consistent with the quaternary ammonium salts that we have characterized and reported previ-

ously.³ An (E,Z)-endo allylic phosphonium bromide is produced exclusively, with no evidence of an exomethylene isomer analogous to **1a** being found in the model or BIIR substitution products (Figure 1). ^{31}P and ^1H NMR analyses of the phosphonium salt of BIIR (IIR- PPh_3Br) confirmed that it is structurally consistent with the model compound. However, notable differences in ^1H NMR line widths were observed for allylic methylene group resonances. These are due to ion-pair aggregation effects, which will be discussed following an account of the synthesis and solid-state properties of these materials. We note that distribution of ionic functionality within IIR- PPh_3Br is expected to be random, given the composition distribution of BIIR.

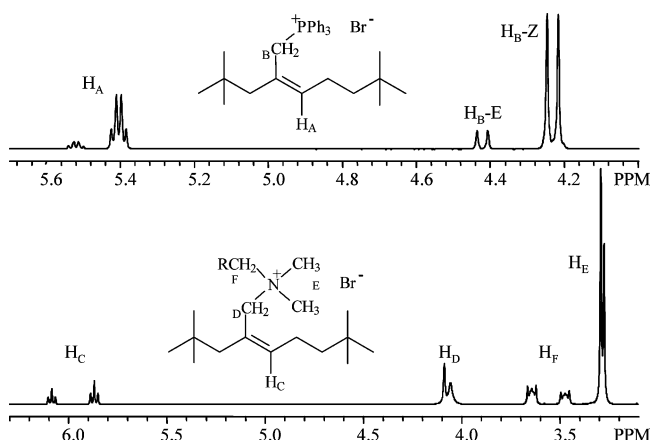


Figure 1. Downfield region of ^1H NMR spectra of model compounds (CDCl_3).

IIR- PPh_3Br . Ionic derivatives of BIIR can be prepared by solvent-free compounding of the elastomer with PPh_3 at elevated temperatures. The allylic bromide content of BIIR places an upper limit on the attainable ion pair concentration, which in the present case was 0.20 mmol/g of polymer. This is comparable to many ionomer systems,⁹ and significant changes to rheological properties are expected if quantitative conversion of BIIR to IIR- PPh_3Br is achieved. However, HBr elimination competes with nucleophilic substitution to affect reaction yields, and a complete understanding of the dynamics of this process requires both rheological and composition data. Therefore, we have assessed the dynamic properties and the composition of reaction mixtures concurrently by conducting alkylation reactions within an oscillating die rheometer. On-line rheological measurements of G' , G'' , and $\tan \delta$ were combined with composition information derived from off-line ^1H NMR analysis to generate the results presented in Figures 2–5.

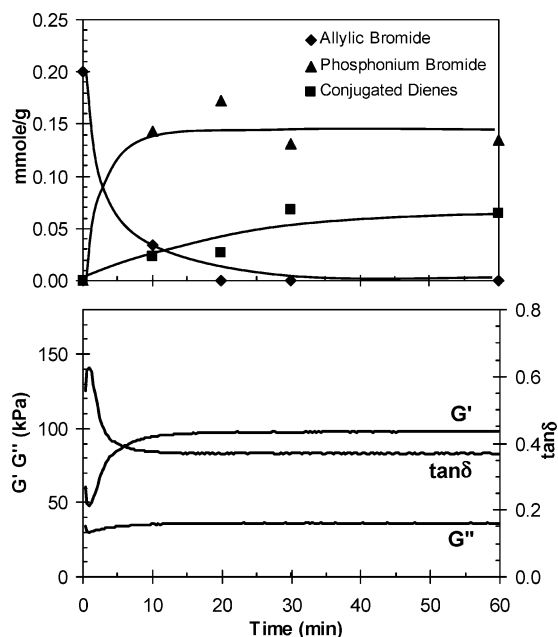


Figure 2. Evolution of reaction products and dynamic properties (3.0 equiv of PPh_3 ; 140 °C; \blacklozenge , 1; \blacksquare , 2; \blacktriangle , 4).

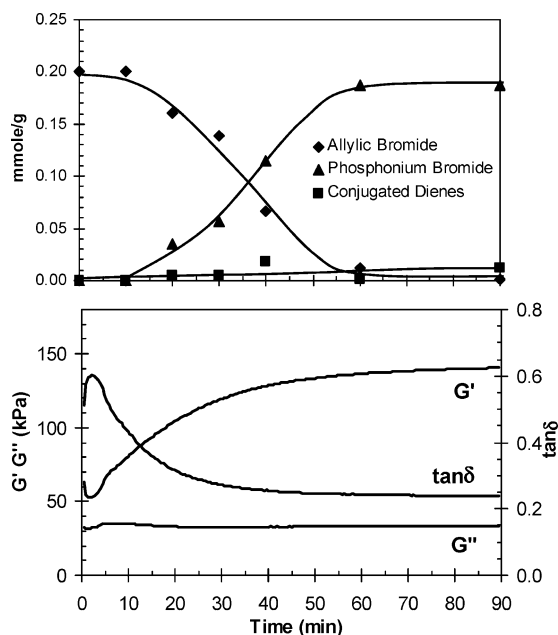


Figure 3. Evolution of reaction products and dynamic properties (3.0 equiv of PPh_3 ; 100 °C; \blacklozenge , 1; \blacksquare , 2; \blacktriangle , 4).

The dynamics of BIIR derivatization at 140 °C are illustrated in Figure 2. Using a 3-fold excess of PPh_3 , quantitative consumption of allylic bromide was realized within 20 min, resulting in a phosphonium bromide yield of 85%. Dehydrobromination products analogous to **2a–c** accounted for the remaining 15% of the product distribution, and HBr liberated by this process was scavenged by the epoxide stabilizers that are added during BIIR manufacturing for this purpose. As expected, the storage modulus (G') increased in direct proportion with the extent of alkylation, resulting in a corresponding decline of $\tan\delta$. We note that a conventional ZnO cure of BIIR yielded comparable rheological properties ($G' = 128$ kPa, $G'' = 24.3$ kPa, $\tan\delta = 0.19$) by generating a vulcanized network of carbon–carbon cross-links.¹⁰ Although a network of similar mechanical strength was generated within IIR- PPh_3Br , the ionomer

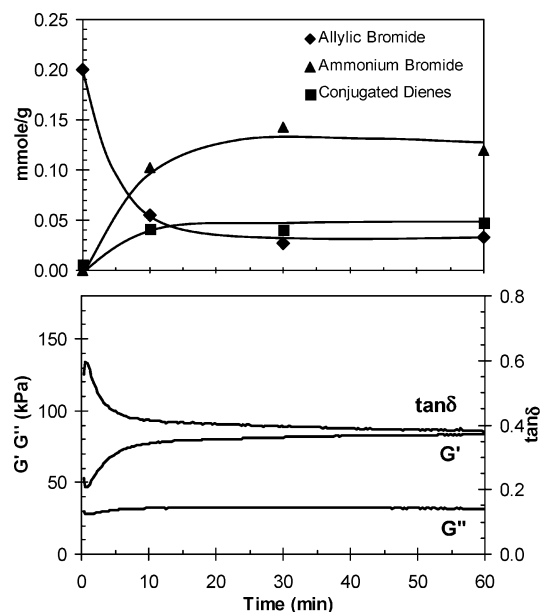


Figure 4. Evolution of reaction products and dynamic properties (4.0 equiv of DMOA; 140 °C; \blacklozenge , 1; \blacksquare , 2; \blacktriangle , 3).

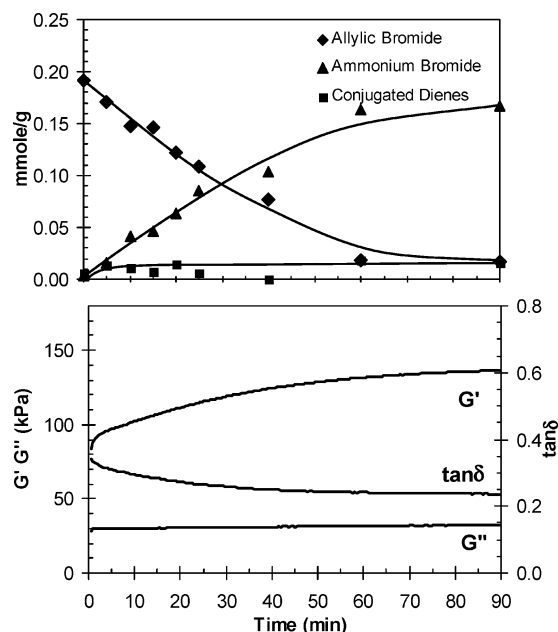


Figure 5. Evolution of reaction products and dynamic properties (4.0 equiv of DMOA; 100 °C; \blacklozenge , 1; \blacksquare , 2; \blacktriangle , 3).

dissolved completely in chloroform, toluene, and hexanes. This suggests that improvements to the complex modulus of the elastomer are due to aggregation of pendant phosphonium bromide groups to yield an extended network of ion-pair multiplets.⁹

Bromide displacement by 3.0 equiv of PPh_3 at 100 °C is illustrated in Figure 3. At this reduced temperature, the rates of alkylation and HBr elimination decreased such that the quantitative consumption of allylic bromide required 60 min. However, a decelerated reaction rate was accompanied by an improvement in selectivity, as the yield of IIR- PPh_3Br increased relative to that of the conjugated dienes derived from dehydrobromination. An experiment conducted with just 1.0 equiv of PPh_3 at 100 °C (not shown) resulted in a lower rate of phosphonium salt production. This is the expected result for a bimolecular nucleophilic substitution, wherein a

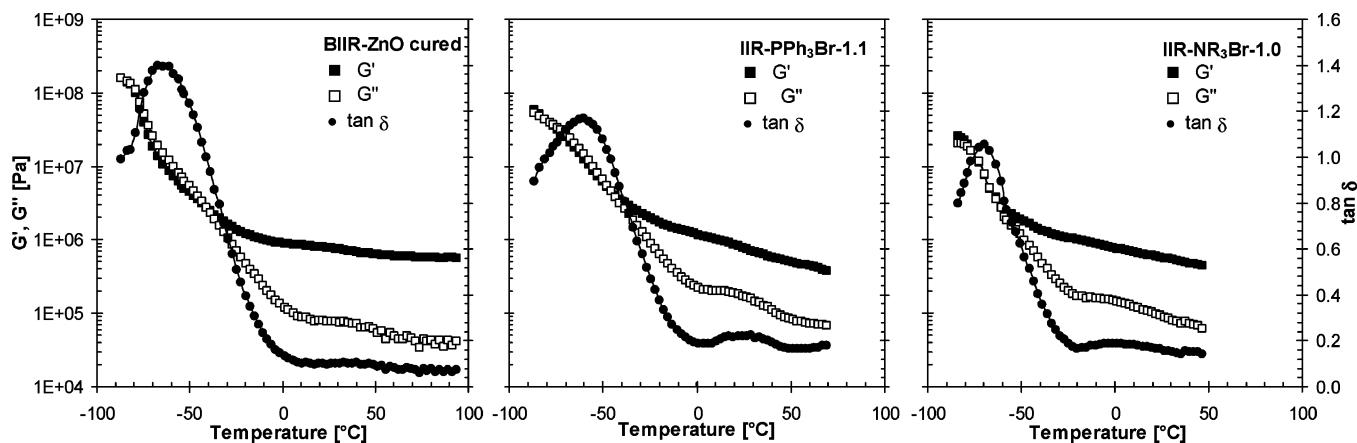


Figure 6. Storage, loss, and phase angle data for ZnO-cured BIIR, IIR-PPh₃Br-1.1, and IIR-NR₃Br-1.0 as a function of temperature (1 Hz, 1° strain).

decrease in the nucleophile concentration reduces the alkylation rate. The dehydrobromination rate was unchanged.

IIR-NR₃Br. In terms of the relationship between ion-pair concentration and solid-state rheological properties, the BIIR/DMOA system is consistent with the BIIR/PPh₃ system. However, important differences exist between the stability of the ammonium bromide functionality within IIR-NR₃Br and its phosphonium analogue. While the substitution of bromide by PPh₃ is irreversible, the reaction of BIIR with DMOA is equilibrium-limited (Figure 4) because of the reversibility of N-alkylation.³ This leads to incomplete conversion of allylic bromide to IIR-NR₃Br and an inherent instability of this product. Although HBr elimination is slower than N-alkylation, the conjugated dienes (**2**) are more stable than the tetralkylammonium bromide salt (**3**). Therefore, N-alkylation reactions progress toward a state that is dominated by **2** and HNR₃Br. In the solid-state preparation used throughout this work, the instability of IIR-NR₃Br was overcome by using a relatively large excess of amine. However, we found that reactions in toluene solutions could not be driven to high conversion using this strategy, since the dilution of an addition reaction such as BIIR + NR₃ ⇌ IIR-NR₃Br displaces the equilibrium position toward the reactants.

Figure 5 illustrates the behavior of the BIIR/DMOA system at 100 °C with 4.0 equiv of amine. The N-alkylation rate is reduced considerably at this temperature, but the overall selectivity for IIR-NR₃Br production vs dienes analogous to **2a–c** is enhanced. Lowering the DMOA loading to 1.0 equiv at 100 °C (not shown) reduced the alkylation rate proportionally.

Solid-State Viscoelastic Properties. The dynamic mechanical properties of IIR-PPh₃Br and IIR-NR₃Br are presented in Figure 6 as a function of temperature. The behavior of a ZnO-cured sample of BIIR is included as a control material for comparative analyses between the ionomers and a nonionic, cross-linked polymer network. The data show only minor differences between the *T_g*'s of IIR-PPh₃Br and ZnO-cured BIIR. However, residual amine within the ammonium bromide ionomer appears to have plasticized the bulk polymer matrix to a small degree, lowering the *T_g* from −64 to −70 °C.

In addition to the glass transition, loss modulus measurements reveal a secondary transition at 35 °C for the control ZnO-cured compound, at 25 °C for IIR-PPh₃Br, and at 0 °C for IIR-NR₃Br. Modulated DSC analyses (not shown) provided no evidence of heat

effects associated with these transitions, and their origin cannot be specified at the present time. However, we note that Charlier et al. observed similar responses of *G'* from quaternary ammonium telechelic polyisoprene samples and attributed them to the disintegration of ionic aggregates.¹¹ Similar changes to chain mobility with temperature may be operative in the present system, although the existence of the transition in the nonionic control compound suggests that further studies are required.

Solution Properties: Viscosity. It is widely recognized that ion-pair aggregation persists when ionomers are dissolved in solvents of low polarity,¹² and these associations lead to complex viscosity–concentration relationships that depend on the dielectric constant of the solvent¹³ as well as the nature of the ionic functionality.¹⁴ Figure 7 presents the viscosity of BIIR, IIR-PPh₃Br, and IIR-NR₃Br solutions in toluene and chloroform. In the dilute region (below 1.0 g/dL), the ionomer viscosities recorded in a given solvent are less than those measured for equivalent BIIR solutions. Given that molecular weight is unchanged when HBr is sequestered effectively during nucleophilic substitutions of BIIR,¹⁵ the observed viscosity reductions are not attributed to polymer degradation but to intramolecular ion-pair association.^{12,16} This is consistent with light¹⁷ and neutron¹⁸ scattering studies of sulfonated polystyrene ionomers, in which ion-pair aggregation is shown to affect solution viscosity by reducing the radius of gyration of ionomer chains.

Although neither chloroform ($\epsilon = 4.81$) nor toluene ($\epsilon = 2.37$) is considered polar, their ability to affect intramolecular ion-pair aggregation differed markedly, as revealed by the intrinsic viscosities [η] recorded in each medium (Figure 7). When dissolved in the more polar of the two solvents (chloroform), the ionomers yielded slightly lower [η] values than their nonionic, parent material. However, intrinsic viscosities differed considerably when these materials were dissolved in toluene. Whereas, the intrinsic viscosity of BIIR in toluene was 1.19 dL/g, IIR-NR₃Br yielded a value of just 0.28 dL/g.

The semidilute regions of Figure 7 (2.0–12.0 g/dL) reveal important differences in the critical entanglement concentrations (*C*^{*}) that mark the point where intermolecular interactions result in grossly elevated solution viscosity.^{19,20} For BIIR, the transition from a state of minimal polymer chain interaction to an entangled state was virtually independent of the solvent. In contrast,

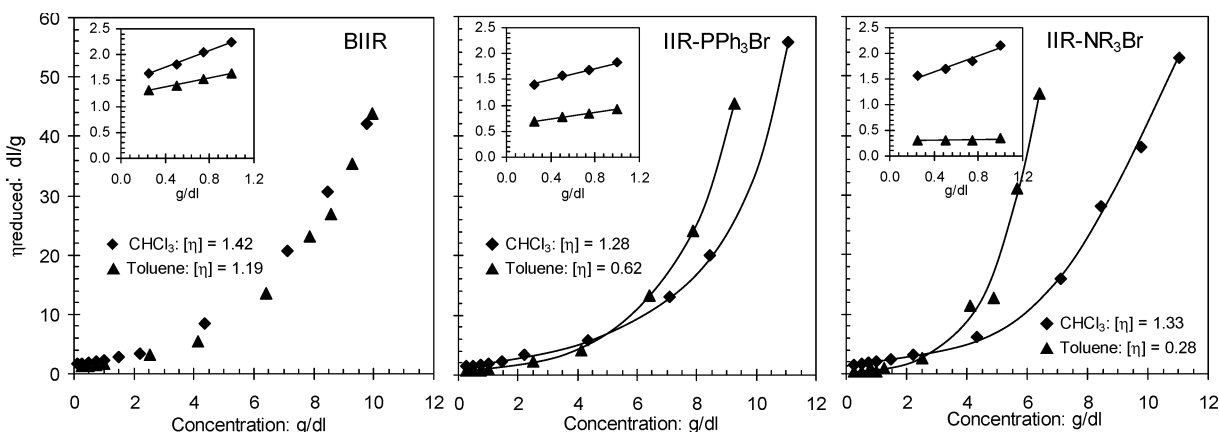


Figure 7. Reduced solution viscosity of BIIR, IIR-PPh₃Br-1.1, and IIR-NR₃Br-0.9 (inset: expansion of low concentration region; 27 °C).

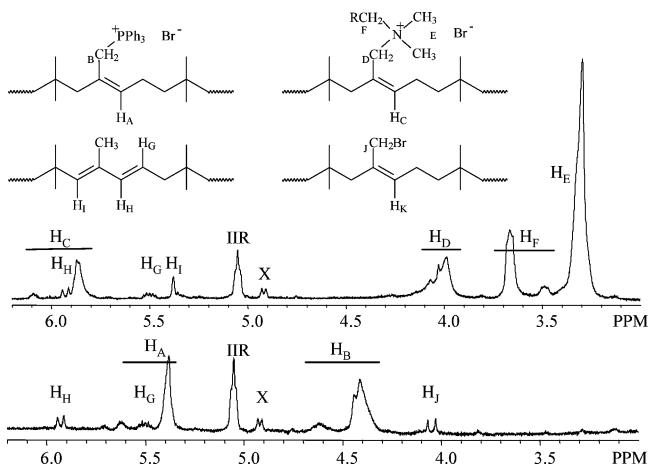


Figure 8. Downfield regions of ¹H NMR spectra of IIR-PPh₃Br and IIR-NR₃Br (CDCl₃).

dominant interchain associations were realized at relatively low concentrations of ionomer, and the onset of these effects was highly sensitive to solvent polarity. The most dramatic example is drawn from the IIR-NR₃Br system, which exhibited remarkable reductions in C^* on moving from chloroform to toluene. Given that the backbone of all three polymers is identical, lower critical entanglement concentrations can be attributed to the strength of intermolecular ion-pair aggregation.²¹ We believe that the model of Lantman et al.¹⁸ may apply to the present case, since it is likely that individual chains retain their dimensions as the polymer concentration is increased toward the critical threshold. Large-scale chain interactions may be assisted by ion-pair association, leading to earlier onsets of chain entanglement.

The large difference between the entanglement concentrations of IIR-NR₃Br and IIR-PPh₃Br in toluene is particularly interesting. We speculate that toluene may solvate quaternary phosphonium bromide multiplets better than ammonium analogues, thereby displacing the onset of chain entanglement to higher concentration in the IIR-PPh₃Br system.¹⁴

Solution Properties: ¹H NMR Spin-Spin Relaxation. Unique relaxation behavior in IIR-PPh₃Br and IIR-NR₃Br solutions is immediately apparent in the ¹H NMR spectra of these materials. Both demonstrate broadness in their downfield allylic methylene resonances (Figure 9) that is not found in the isobutylene-based backbone signals or in the spectra of model

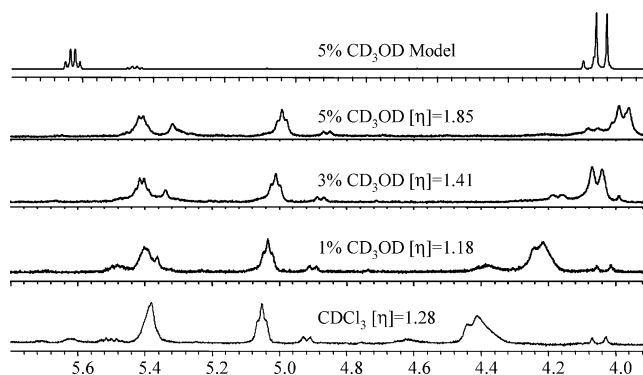


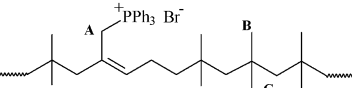
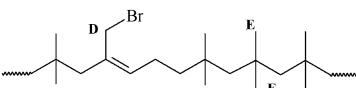
Figure 9. Downfield ¹H NMR spectra of IIR-PPh₃Br-1.1 and its model compound analogue in chloroform-methanol solutions.

compound analogues (Figure 1). Broad line widths are often cited as evidence of reduced functional group mobility, given the close relationship between spin-spin relaxation times (T_2) and the correlation frequency for molecular reorientation.²² Since the latter is directly related to the rate of molecular tumbling, T_2 /line width measurements have been used to demonstrate reduced mobility of sulfonate groups within Nafion²³ and of metal carboxylate groups within polybutadiene-based ionomers.²⁴ Since the allylic methylene group resonances adjacent to the phosphonium bromide functionality are well-resolved from those of the polymer backbone, the extent to which the ionic functionality of this material incurs specific mobility restrictions was probed by relaxation measurements.

We have limited our relaxation studies to IIR-PPh₃Br since the IIR-NR₃Br system presents additional complications derived from chemical exchange and the scalar contributions of quadrupolar nitrogen. ³¹P NMR experiments confirmed that phosphine exchange does not occur rapidly enough (if at all) to affect relaxation in IIR-PPh₃Br-chloroform solutions. The addition of free PPh₃ to a CDCl₃ solution of IIR-PPh₃Br produced an NMR spectrum comprised of the precise chemical shifts for PPh₃ (δ -4.5 ppm) and the polymer (δ 22.25, 19.84 ppm). Moreover, a 2-dimensional ³¹P NOESY experiment revealed no interaction between free and bound phosphine. Therefore, we are confident that the broadness of allylic phosphonium bromide resonances is due to efficient spin-spin relaxation of this functionality.

Inversion-recovery and spin-echo experiments were used to determine spin-lattice (T_1) and spin-spin (T_2)

Table 1. ^1H NMR Relaxation Parameters

	CDCl ₃		CDCl ₃ 3% CD ₃ OD	
	T ₁ : ms	T ₂ : ms	T ₁ : ms	T ₂ : ms
H _A	144	45	294	82
H _B	240	192	237	188
H _C	240	157	239	161
H _D	427	169	402	170
H _E	236	204	232	187
H _F	237	165	236	158
				
* polymer concentration = 1.42 g/100 ml				
** IIR-PPh ₃ Br-1.1				

relaxation times for the principal resonances of BIIR and IIR-PPh₃Br (Table 1). One set of characteristic relaxation times (T_1 and T_2) was capable of representing the decay of each resonance, which confirms that each nucleus experiences a single environment in a homogeneous solution. Comparisons of spin–spin relaxation constants between IIR-PPh₃Br and BIIR revealed no significant differences between the T_2 values of isobutylene resonances. Therefore, these elements of the chain have similar local mobility in both polymers. However, the T_2 of the allylic resonances of IIR-PPh₃Br (**4**) were much shorter than the corresponding resonances of the exo-allylic bromide (**1b**), indicating that the $-\text{CH}_2-\text{PPh}_3\text{Br}$ system relaxes more efficiently than the $-\text{CH}_2-\text{Br}$ system. While these differences between IIR-PPh₃Br and BIIR may be rationalized using chain mobility arguments, we believe that more conclusive evidence of specific ion-pair mobility restrictions is provided examining the effect of methanol on relaxation behavior and intrinsic viscosity.

The capacity of alcohols to affect sulfonate group associations in polystyrene-based ionomers is widely recognized and has been well characterized by small-angle neutron scattering,²⁵ dilute solution viscosity,¹³ and electron spin resonance²⁶ studies of this material. ^{19}F NMR line width analysis has been employed for the study of perfluorsulfonate ionomers, in which alcohol-swollen samples revealed evidence of selective increases in ion-pair mobility relative to the polymer backbone.²⁷ Our relaxation studies of the influence of methanol on IIR-PPh₃Br/chloroform solutions have produced similar conclusions. Figure 9 provides ^1H NMR and $[\eta]$ data for the ionomer as a function of increasing CD_3OD concentration. Greater mobility of phosphonium bromide functionality is indicated by the reduced line width of $-\text{CH}_2-\text{PPh}_3\text{Br}$ resonances. The T_2 relaxation times for these resonances increased from 45 ms in pure CDCl_3 to 82 ms in 3% $\text{CD}_3\text{OD}/\text{CDCl}_3$ solution, while the relaxation of isobutylene-based resonances was unaffected by the presence of alcohol (Table 1). Moreover, the chemical shifts of the allylic phosphonium bromide resonances derived from IIR-PPh₃Br evolved toward those of the model compound as methanol was charged to the system. This suggests that the environment about ion pairs is more closely matched as intramolecular aggregation effects are reduced.

Viscosity measurements of IIR-PPh₃Br in chloroform/methanol solutions revealed a steady increase in intrinsic viscosity as methanol concentrations were increased (Figure 9). This is further evidence of a reduction in the

extent of intramolecular ion-pair aggregation, which is consistent with NMR relaxation measurements that showed improvements in ion-pair mobility. This link between phosphonium bromide functional group mobility and solution viscosity confirms that ionic aggregation is the source of the bulk property variations brought about by bromide displacement from BIIR by phosphine and amine nucleophiles.

Conclusions

The quaternization of PPh₃ and DMOA by reaction with BIIR produces elastomeric ionomers whose mechanical properties are comparable to ZnO-cured vulcanizates. Dynamic mechanical analysis as well as solution viscosity and ^1H NMR relaxation studies confirm that ion-pair aggregation establishes a thermoplastic network whose strength is dependent upon temperature and the presence of selective plasticizers.

Acknowledgment. Financial support from the Centre for Automotive Materials and Manufacturing (Camm) and from Bayer Polymers is gratefully acknowledged.

References and Notes

- (1) (a) Kennedy, J. P.; Ross, L. R.; Lackey, J. E.; Nuyken, O. *Polym. Bull. (Berlin)* **1981**, *4*, 67–74. (b) Kennedy, J. P.; Storey, R. F. *Am. Chem. Soc. Div. Org. Coat. Appl. Polym. Sci.* **1981**, *46*, 182–185. (c) Canter, N. H.; Kennedy, J. P. United States Patent 3646166, 1972.
- (2) (a) Parent, J. S.; White, G.; Whitney, R. A. *J. Polym. Sci., Part A: Polym. Chem.* **2002**, *40*, 2937–2944. (b) Parent, J. S.; White, G. D. F.; Thom, D. J.; Whitney, R. A.; Hopkins, W. *J. Polym. Sci., Part A: Polym. Chem.* **2003**, *41*, 1915–1926.
- (3) Parent, J. S.; White, G. D. F.; Whitney, R. A.; Hopkins, W. *Macromolecules* **2002**, *35*, 3374–3379.
- (4) Arjunan, P.; Wang, H. C. *Polym. Mater. Sci. Eng.* **1997**, *76*, 310–311.
- (5) Antony, P.; De, S. K. *J. Macromol. Sci., Polym. Rev.* **2001**, *C41*, 41–77.
- (6) Parent, J. S.; Thom, D. J.; White, G.; Whitney, R. A.; Hopkins, W. *J. Polym. Sci., Part A: Polym. Chem.* **2001**, *39*, 2019–2026.
- (7) Huggins, M. L. *J. Am. Chem. Soc.* **1942**, *64*, 2716–2718.
- (8) Chu, C. Y.; Vukov, R. *Macromolecules* **1985**, *18*, 1423–1430.
- (9) (a) *Ionic Polymers*; Halliday, L., Ed.; Wiley: New York, 1975. (b) *Introduction to Ionomers*; Eisenberg, A., Kim, J. S., Eds.; Wiley: New York, 1998.
- (10) Vukov, R. *Rubber Chem. Technol.* **1984**, *57*, 284–290.
- (11) Charlier, P.; Jerome, R.; Teyssie, P.; Utracki, L. A. *Macromolecules* **1992**, *25*, 617–624.
- (12) Lundberg, R. D.; Phillips, R. R. *J. Polym. Sci., Polym. Phys. Ed.* **1982**, *20*, 1143–1154.

- (13) Lundberg, R. D.; Makowski, H. S. *J. Polym. Sci., Polym. Phys. Ed.* **1980**, *18*, 1821–1836.
- (14) Hara, M.; Lee, A. H.; Wu, J. *J. Polym. Sci., Part B: Polym. Phys.* **1987**, *25*, 1407–1418.
- (15) Dehydrobromination can lead to cationic oligomerization and fragmentation reactions when HBr is not scavenged by base and/or epoxides.
- (16) Hara, M.; Wu, J. L.; Lee, A. H. *Macromolecules* **1988**, *21*, 2214–2218.
- (17) (a) Lantman, C. W.; MacKnight, W. J.; Peiffer, D. G.; Sinha, S. K.; Lundberg, R. D. *Macromolecules* **1987**, *20*, 1096–1101. (b) Hara, M.; Wu, J. L. *Macromolecules* **1988**, *21*, 402–407. (c) Pedley, A. M.; Higgins, J. S.; Peiffer, D. G.; Burchard, W. *Macromolecules* **1990**, *23*, 1434–1437.
- (18) Lantman, C. W.; MacKnight, W. J.; Higgins, J. S.; Peiffer, D. G.; Sinha, S. K.; Lundberg, R. D. *Macromolecules* **1988**, *21*, 1339–1343.
- (19) Wang, C. S.; Fried, J. R. *J. Rheol.* **1992**, *36*, 929–945.
- (20) Lundberg, R. D. *J. Appl. Polym. Sci.* **1982**, *27*, 4623–4635.
- (21) Broze, G.; Jerome, R.; Teyssie, P.; Marco, C. *Macromolecules* **1983**, *16*, 996–1000.
- (22) (a) Yoshimizu, H.; Tsujita, Y. *Ann. Rep. NMR Spectrosc.* **2001**, *44*, 1–22. (b) Ruytinx, B.; Berghmans, H.; Andriaenssens, P.; Storme, L.; Vanderzande, D.; Gelan, J.; Paoletti, S. *Macromolecules* **2001**, *34*, 522–528. (c) Gao, Z.; Zhong, X. F.; Eisenberg, A. *Macromolecules* **1994**, *27*, 794–802.
- (23) Schlick, S.; Gebel, G.; Pineri, M.; Volino, F. *Macromolecules* **1991**, *24*, 3517–3521.
- (24) (a) McBrierty, V. J.; Douglass, D. C.; Zhang, X.; Quinn, F. X.; Jerome, R. *Macromolecules* **1993**, *26*, 1734–1739. (b) Vanhoorne, P.; Jerome, R.; Teyssie, P.; Laupretre, F. *Macromolecules* **1994**, *27*, 2548–2552.
- (25) Pedley, A. M.; Higgins, J. S.; Peiffer, D. G.; Rennie, A. R. *Macromolecules* **1990**, *23*, 2494–2500.
- (26) Weiss, R. A.; Fitzgerald, J. J.; Kim, D. *Macromolecules* **1991**, *24*, 1064–1070.
- (27) (a) Meresi, G.; Wang, Y.; Bandis, A.; Inglefield, P. T.; Jones, A. A.; Wen, W.-Y. *Polymer* **2001**, *42*, 6153–6160. (b) Giotto, M. V.; Zhang, J.; Inglefield, P. T.; Wen, W.-Y.; Jones, A. A. *Macromolecules* **2003**, *36*, 4397–4403.

MA049158K